Title

Analytical Modeling of AdHoc Networks that Utilize Space-Time Coding

Author

Garcia-Luna-Aceves, J.J.

Publication Date

2006-04-03

Peer reviewed

Analytical Modeling of Ad Hoc Networks that Utilize Space-Time Coding

Marcelo M. Carvalho
* Computer Engineering Department
University of California Santa Cruz
Santa Cruz, CA 95064 USA
carvalho@soe.ucsc.edu

J. J. Garcia-Luna-Aceves *†
† Palo Alto Research Center
3333 Coyote Hill Road
Palo Alto, CA 94304 USA
jj@soe.ucsc.edu

***Abstract*— This paper presents the first analytical model for ad hoc networks equipped with multiple-input multiple-output (MIMO) radios using space-time coding (STC) that considers the impact of the underlying radio-based topology on network performance. In particular, we consider the space-time block coding (STBC) technique known as the "Alamouti scheme." We derive the effective signal-to-interference-plus-noise density ratio (SINR) of the Alamouti scheme under multiple access interference (MAI), and we propose the moment generating function (MGF) method to derive closed-form expressions for its symbol error probability under different modulation schemes when fading paths are independent but not necessarily identically distributed. The impact of the Alamouti scheme on IEEE 802.11 ad hoc networks is studied by introducing a new analytical model for the IEEE 802.11 DCF MAC. The model we introduce takes into account the impact of errors in both control and data frames, the carrier-sensing activity, and the finite-retry limit of frame retransmissions. Both PHY- and MAC-layer analytical models are incorporated into our previously-designed, general analytical model for ad hoc networks based on *interference matrices*. We apply the Alamouti scheme to different antenna system configurations and compare their performance with respect to the basic single-input-single-output (SISO) IEEE 802.11 DCF MAC.**

I. Introduction

Recent information-theoretic results [1], [2], [3], [4] have shown that large gains in communication capacity over wireless channels can be obtained if multiple antenna elements are used in both ends of the wireless link—the so-called *multiple-input multiple-output (MIMO) systems*. As a consequence, MIMO technology has emerged as one of the most promising fields in modern communications with a chance to resolve the bottleneck capacity of future high-demand wireless networks [5], [6].

In practice, however, achieving the high capacity gains promised by theory requires the development of algorithms and signal design/processing techniques that are able to trade off system complexity with performance (the theory only provides performance bounds based on algorithms/codes with unbounded complexity or latency [5]). One such set of practical signal design techniques is *space-time coding* (STC) [7], [8]. As the name suggests, STC exploits both temporal and spatial dimensions inherent in the use of multiple spatially-distributed antennas to design codes that aim to achieve the capacity limits of MIMO channels. In the *space-time encoder*, code symbols are generated and transmitted simultaneously from each antenna in a way that *diversity*, *array*, and/or *coding* gains can be obtained under high spectral efficiency with the use of appropriate signal processing and decoding procedures at the receiver.

Despite the enormous advantages envisaged with the use of MIMO technology, to date, the majority of the work in ad hoc networks equipped with multiple antennas has focused on solutions in which the primary goal is to obtain a more reliable communication link by focusing energy into desired directions ("directional antennas"). So far, very few works have attempted to integrate MIMO systems into ad hoc networks, and little is known about the impact of such technology on the performance of ad hoc networks under specific medium access control (MAC) protocols. Section II reviews the prior work on MIMO ad hoc networks.

Although a cross-layer design approach to both physical (PHY) and MAC layers is likely to obtain the most benefit out of MIMO technology, it is important to know what is the impact of MIMO on the performance of ad hoc networks *if the MAC layer is kept intact*. In fact, such separation of roles may be unavoidable in many cases (e.g., the IEEE 802.11 standard states that [9, pp. 149] "the architecture of the IEEE 802.11 MAC is intended to be PHY independent."). Accordingly, this paper attempts to address the following questions by introducing the first analytical model of MIMO ad hoc networks with *specific* PHY and MAC layers:

1) How do the PHY improvements provided by a *specific* MIMO technology reflect on overall network performance for a *given* MAC protocol?
2) Are the gains significant enough to justify the added complexity and processing cost incurred by the MIMO technology?
3) How do the performance gains obtained with *multiple-input single-output* (MISO) or MIMO systems compare to the simplest *single-input single-output* (SISO) case?
4) What are the relative gains in performance as the number of antenna elements increases?

We investigate the impact of *space-time block codes* (STBC) [10] in ad hoc networks operating with the IEEE 802.11 DCF MAC. For the STBC, we investigate the use of the Alamouti scheme [11], which is currently part of both W-

0-7803-9550-6/06/$20.00 © 2006 IEEE

CDMA and CDMA-2000 standards. Among its advantages, the Alamouti scheme supports maximum-likelihood detection based only on linear processing at the receiver and it does not require channel state information (CSI) at the transmitter. Section III-A describes the basics of the Alamouti scheme, with an example of a MIMO system with two transmit antennas and two receive antennas. Section III-B derives the effective signal-to-interference-plus-noise density ratio (SINR) of the Alamouti scheme under multiple access interference (MAI), which is key for the performance of Alamouti-enabled MIMO ad hoc networks. Also, Section III-C proposes the use of the moment generating function (MGF) method to derive closed-form expressions for the symbol error probability of the Alamouti scheme under different modulation schemes when fading paths are independent but not necessarily identically distributed.

For the analytical modeling of ad hoc networks, we use our previous results [12], [13], which provide an analytical framework that captures the interactions between the PHY and MAC layers while taking into account the radio connectivity among the nodes—all conveniently conveyed through the use of *interference matrices*. Section IV reviews the basic facts of our modeling approach.

Section V introduces a new Markov model for the operation of the IEEE 802.11 DCF MAC that includes the impact of the carrier-sensing activity, the finite-retry limit of frame retransmissions, and takes into account the impact of errors in both control and data frames (assuming the four-way handshake mechanism). Previous models have explicitly assumed perfect channel conditions (i.e, no channel errors, no hidden terminals, etc.). Consequently, the only reason for errors to occur were assumed to be due to RTS collisions at a receiver, when two or more nodes attempted to transmit at the same time (disregarding, thus, the capture phenomenon). Our new model, instead, includes the impact of errors in both control and data frames on the dynamics of the IEEE 802.11 DCF MAC. In Section VI we validate our model, showing that it can predict simulation results very accurately, with processing times that are orders of magnitude faster than simulations.

Section VII incorporates the impact of the Alamouti scheme into IEEE 802.11 ad hoc networks. Because of its flexibility, we study the use of Alamouti scheme in MISO and MIMO ad hoc networks, comparing their relative performance with respect to SISO networks. Section VIII summarizes our conclusions.

II. Related Work

So far, not much work has been done on MIMO ad hoc networks. Sundaresan *et al.* [14] introduced a distributed MAC protocol for MIMO links based on a centralized MAC that applies spatial multiplexing assuming closed-loop MIMO and ideal interference cancellation. Tang *et al.* [15] proposed the design of a new transceiver based on a space-time interference canceling technique for MIMO-OFDM, and a MAC protocol (MIMA-MAC) that takes advantage of their transceiver capability in demodulating multiple data streams. Park *et al.* [16] designed a MAC protocol (SPACE-MAC) for MIMO links based on MIMO *beamforming*, i.e., a MIMO technique by which the same symbol is transmitted from each antenna according to a pre-selected weighting scheme[1]. At demodulation, appropriate weights are selected at the receive antennas to recover the transmitted symbol. SPACE-MAC selects the weights in such a way that simultaneous transmissions may occur among nodes within range of each other, improving the spatial reuse.

Regarding the use of space-time coding in ad hoc networks, Stamoulis and Al-Dhahir [17] investigated the impact of space-time block codes on IEEE 802.11a wireless local area networks (WLANs) operating in ad hoc mode. They used simulations to assess the benefits of the Alamouti scheme on the performance of upper-layer protocols like TCP. Their work assumes fully-connected networks (i.e., no hidden terminals) and focuses on the simplest Alamouti scheme, i.e., a MISO system with two transmit antennas and one receive antenna.

Hu and Zhang [18] attempted to model MIMO ad hoc networks by focusing on IEEE 802.11 ad hoc networks operating with STBC. For the modeling of the IEEE 802.11 DCF MAC, they used the same Markov model as the one introduced by Bianchi [19], which does not include the impact of the finite-retry limits or the carrier-sensing activity of the nodes, and assumes that collisions occur only among RTS frames. In addition, they disregarded the impact of the network topology, and assumed that "events experienced by one user are statistically the same as those of other users," stating that each node has the *same* average throughput. In fact, in their model, each node is surrounded by the same average number of nodes, and the multihop network simplifies, in practice, to many "single-hop" networks, where interactions happen only with *immediate* neighbors. Therefore, their model ignores the impact of the topology and the radio connectivity among all nodes in the network. Consequently, it does not capture the interactions between PHY and MAC layers, which is key for an accurate evaluation of the impact of any PHY-layer aspect on the performance of a multihop network.

III. Space-Time Coding (STC)

The fundamentals of space-time coding (STC) were first established by Tarokh *et al.* [7] who proposed *space-time trellis codes* (STTC). STTC is an extension of standard trellis codes to MIMO systems, with the difference that the decoding procedure of STTC requires multidimensional Viterbi algorithms at the receiver. They designed codes that attain a diversity order equal to the number of transmit antennas, and a coding gain that depends on the complexity of the code (i.e., number of states in the trellis) without incurring any loss in bandwidth efficiency. Unfortunately, a major drawback of STTC is the fact that the decoding complexity increases exponentially as a function of the diversity level and transmission rate.

[1]The term "beamforming" is also used in the context of smart antennas to describe the adjustment of the antenna weights to *direct* the antenna beam in a given direction.

Later, Alamouti [11] proposed a space-time block coding (STBC) scheme for transmission with two antennas that supports maximum-likelihood detection based only on linear processing at the receiver. In addition, the Alamouti scheme does not require any channel feedback from the receiver to the transmitter (the channel is unknown to the transmitter) and it does not incur any bandwidth expansion. The basic Alamouti scheme consists of two transmit antennas and one receive antenna (MISO system), but it can be easily generalized to the case of two transmit antennas and M receive antennas to provide a diversity order of $2M$. Tarokh *et al.* [10] generalized this scheme to an arbitrary number of transmit antennas. In this paper, however, we focus on systems with two transmit antennas and M receive antennas.

Next, we present a short overview of the basics of the Alamouti scheme applied to a MIMO system with two transmit antennas and two receive antennas. Following that, we compute the impact of multiple access interference (MAI) in an ad hoc network operating with the Alamouti scheme, and show a simple way to compute the symbol error probability of the Alamouti scheme under multipath fading.

A. Example: The 2 × 2 MIMO Alamouti Scheme

The Alamouti scheme [11] works over two symbol periods. Over the first symbol period, two different symbols s_1 and s_2 are transmitted simultaneously from antennas 1 and 2, respectively. During the next symbol period, symbol $-s_2^*$ is transmitted from antenna 1, and symbol s_1^* is transmitted from antenna 2 (where * indicates the complex conjugate operation). At each symbol period, the energy E_s available at the transmitter is equally divided between the two antennas, i.e., each symbol has energy $E_s/2$ (no extra power is needed). It is assumed that the channel remains constant over two consecutive symbol periods and it is frequency flat, with $h_{kl} = |h_{kl}|e^{j\theta_{kl}},\ k,l = 1,2$, representing the complex channel gains between the lth transmit antenna and the kth receive antenna. Under such conditions, the 2×2 channel matrix $\mathbf{H}$ is given by

$$\mathbf{H} = \begin{bmatrix} h_{11} & h_{12} \\ h_{21} & h_{22} \end{bmatrix}, \tag{1}$$

and the received signals $\mathbf{y}_1$ and $\mathbf{y}_2$ at the receive antenna array over consecutive symbol periods are given by

$$\mathbf{y}_1 = \begin{bmatrix} h_{11} & h_{12} \\ h_{21} & h_{22} \end{bmatrix} \begin{bmatrix} s_1 \\ s_2 \end{bmatrix} + \begin{bmatrix} n_1 \\ n_2 \end{bmatrix}, \tag{2}$$

$$\mathbf{y}_2 = \begin{bmatrix} h_{11} & h_{12} \\ h_{21} & h_{22} \end{bmatrix} \begin{bmatrix} -s_2^* \\ s_1^* \end{bmatrix} + \begin{bmatrix} n_3 \\ n_4 \end{bmatrix}, \tag{3}$$

where n_1, n_2, n_3, and n_4 are assumed to be uncorrelated AWGN samples with zero mean and power N_0.

The receiver uses the sequentially-received symbols $\mathbf{y}_1$ and $\mathbf{y}_2$ to form the vector $\mathbf{y} = [\mathbf{y}_1\, \mathbf{y}_2^*]^T$, given by

$$\mathbf{y} = \begin{bmatrix} \mathbf{y}_1 \\ \mathbf{y}_2^* \end{bmatrix} = \begin{bmatrix} h_{11} & h_{12} \\ h_{21} & h_{22} \\ h_{12}^* & -h_{11}^* \\ h_{22}^* & -h_{21}^* \end{bmatrix} \begin{bmatrix} s_1 \\ s_2 \end{bmatrix} + \begin{bmatrix} n_1 \\ n_2 \\ n_3^* \\ n_4^* \end{bmatrix} = \mathbf{H}_{\mathrm{A}}\,\mathbf{s} + \mathbf{n}, \tag{4}$$

where $\mathbf{s} = [s_1\ s_2]^T$ and $\mathbf{n} = [n_1\ n_2\ n_3^*\ n_4^*]^T$. By construction, $\mathbf{H}_{\mathrm{A}}$ is orthogonal *irrespective of the channel realization*, i.e., $\mathbf{H}_{\mathrm{A}}^H\mathbf{H}_{\mathrm{A}} = \|\mathbf{H}\|_F^2\mathbf{I}_2$, where $\mathbf{I}_2$ is the 2×2 identity matrix and $\|\mathbf{H}\|_F^2$ is the *frobenius norm* of $\mathbf{H}$, i.e.,

$$\|\mathbf{H}\|_F^2 = \sum_i \sum_j |h_{ij}|^2. \tag{5}$$

By defining the new vector $\mathbf{z} = \mathbf{H}_{\mathrm{A}}^H\mathbf{y}$, one gets

$$\mathbf{z} = \|\mathbf{H}\|_F^2\mathbf{I}_2\,\mathbf{s} + \tilde{\mathbf{n}}, \tag{6}$$

where $\tilde{\mathbf{n}} = \mathbf{H}_{\mathrm{A}}^H\mathbf{n}$ is a complex Gaussian noise vector with $E\{\tilde{\mathbf{n}}\} = \mathbf{0}$, and covariance matrix $E\{\tilde{\mathbf{n}}\tilde{\mathbf{n}}^H\} = \|\mathbf{H}\|_F^2 N_0\mathbf{I}_2$. The diagonal nature of $\mathbf{z}$ effectively decouples the two symbol transmissions, so that each component of $\mathbf{z}$ corresponds to one of the transmitted symbols:

$$z_i = \|\mathbf{H}\|_F^2\, s_i + \tilde{n}_i, \quad i = 1,2. \tag{7}$$

Thus, the received SNR corresponds to the SNR for z_i, which is given by [20]

$$\mathrm{SNR} = \frac{\|\mathbf{H}\|_F^2 E_s}{2N_0}, \tag{8}$$

where the factor of 2 comes from the fact that s_i is transmitted using half of the total energy E_s.

B. Multiple Access Interference (MAI)

In order to model MIMO ad hoc networks properly, we need to characterize the impact of MAI on the signaling technique of choice, taking into account the MIMO nature of the channel. In this section, we consider the impact of MAI in ad hoc networks operating with the Alamouti scheme. Without loss of generality, we consider the simplest Alamouti scheme, which consists of two transmit antennas and one receive antenna (MISO channel). In this case, we assume that every node in the network has two antennas, but only the signals captured by one of the antennas are decoded/demodulated for signal reception.

Let h_{1k}^j and h_{2k}^j denote the complex channel gains between antennas 1 and 2 of node k and the receive antenna of node j, respectively (notice that we have a 1×2 channel matrix in the MISO case). Likewise, let s_{1k} and s_{2k} denote the two symbols transmitted from antennas 1 and 2 of node k. Now, let us assume that node i transmits a signal to node j and that other K nodes are transmitting simultaneously over the channel (not necessarily to node j). Therefore, the signals y_1^j and y_2^j received by node j over two consecutive symbol periods are given by

$$y_1^j = h_{1i}^j s_{1i} + h_{2i}^j s_{2i} + \underbrace{\sum_{k=1}^{K}\left(h_{1k}^j s_{1k} + h_{2k}^j s_{2k}\right)}_{\text{MAI}}, \tag{9}$$

$$y_2^j = -h_{1i}^j s_{2i}^* + h_{2i}^j s_{1i}^* + \underbrace{\sum_{k=1}^{K}\left(-h_{1k}^j s_{2k}^* + h_{2k}^j s_{1k}^*\right)}_{\text{MAI}}, \tag{10}$$

where, as indicated, the terms under summation form the multiple access interference (MAI) at node j. As explained before, node j constructs the vector $\mathbf{y}_j = [y_1^j \; y_2^{j*}]^T$, leading to

$$\mathbf{y}_j = \begin{bmatrix} h_{1i} & h_{2i} \\ h_{2i}^* & -h_{1i}^* \end{bmatrix} \begin{bmatrix} s_{1i} \\ s_{2i} \end{bmatrix} + \sum_{k=1}^{K} \begin{bmatrix} h_{1k} & h_{2k} \\ h_{2k}^* & -h_{1k}^* \end{bmatrix} \begin{bmatrix} s_{1k} \\ s_{2k} \end{bmatrix}$$
$$= \mathbf{H}_i \, \mathbf{s}_i + \sum_{k=1}^{K} \mathbf{H}_k \, \mathbf{s}_k \quad (11)$$

As in the previous section, it is assumed that node j estimates the channel perfectly from the signals received by node i, i.e., node j has accurate estimates of the channel gains h_{1i}^j and h_{2i}^j. Therefore, node j forms the new vector $\mathbf{z}_j = \mathbf{H}_i^H \mathbf{y}_j$ given by

$$\mathbf{z}_j = \mathbf{H}_i^H \mathbf{H}_i \, \mathbf{s}_i + \sum_{k=1}^{K} \mathbf{H}_i^H \mathbf{H}_k \, \mathbf{s}_k = \|\mathbf{H}_i\|_F^2 \mathbf{I}_2 \, \mathbf{s}_i + \mathbf{m}, \quad (12)$$

where $\mathbf{m}$ is the MAI term given by $\mathbf{m} = \sum_{k=1}^{K} \mathbf{H}_i^H \mathbf{H}_k \, \mathbf{s}_k$. Notice the resemblance between Eqs. (12) and (6). Assuming that the symbols are equally probable and drawn from a symmetric constellation, then $E\{\mathbf{m}\} = \mathbf{0}$. For the covariance matrix $E\{\mathbf{m}\mathbf{m}^H\}$, we have

$$E\{\mathbf{m}\mathbf{m}^H\} = E\left\{ \left(\sum_{k=1}^{K} \mathbf{H}_i^H \mathbf{H}_k \, \mathbf{s}_k \right) \left(\sum_{l=1}^{K} \mathbf{H}_i^H \mathbf{H}_l \, \mathbf{s}_l \right)^H \right\}$$
$$= \sum_{k=1}^{K} \sum_{l=1}^{K} \mathbf{H}_i^H \mathbf{H}_k \, E\{\mathbf{s}_k \mathbf{s}_l^H\} \mathbf{H}_l^H \mathbf{H}_i. \quad (13)$$

If we also make the common assumption that symbols are generated independently at each node, the double summation in Eq. (13) simplifies to

$$E\{\mathbf{m}\mathbf{m}^H\} = \sum_{k=1}^{K} \mathbf{H}_i^H \mathbf{H}_k \, E\{\mathbf{s}_k \mathbf{s}_k^H\} \mathbf{H}_k^H \mathbf{H}_i$$
$$= \sum_{k=1}^{K} \mathbf{H}_i^H \mathbf{H}_k \, \sigma_s^2 \mathbf{I}_2 \mathbf{H}_k^H \mathbf{H}_i = \sigma_s^2 \|\mathbf{H}_i\|_F^2 \sum_{k=1}^{K} \|\mathbf{H}_k\|_F^2 \mathbf{I}_2, \quad (14)$$

where $\sigma_s^2 = E\{s_{1k} s_{1k}^*\} = E\{s_{2k} s_{2k}^*\}$ is the power of the transmitted symbols (remember that they are transmitted with the same power). Hence, as in the previous section, the signal-to-interference-ratio (SIR) for each received symbol corresponds to the SIR for z_i, which is given by

$$\text{SIR} = \frac{\|\mathbf{H}_i\|_F^2 E_s/2}{\sum_k \|\mathbf{H}_k\|_F^2 E_s/2} \quad (15)$$

This last expression tells us that the interference caused by all simultaneous transmissions is nothing but the sum of all the signal powers received by node j from all possible transmit-receive antenna pairs formed between node j and the transmitting nodes. Finally, if we consider both the additive background noise (from previous section) and the MAI, we have the signal-to-interference-plus-noise (SINR) ratio, given by

$$\text{SINR} = \frac{\|\mathbf{H}_i\|_F^2 E_s/2}{N_0 + \sum_k \|\mathbf{H}_k\|_F^2 E_s/2}. \quad (16)$$

C. Symbol Error Probability

The symbol error probability of the Alamouti scheme can be easily obtained if we notice that the received SNR is *the sum of the SNRs from each individual path*[2], i.e., from Eqs. (5) and (8),

$$\text{SNR} = \gamma = \sum_{i=1}^{2} \sum_{j=1}^{M_R} \gamma_{ij} = \sum_{i=1}^{2} \sum_{j=1}^{M_R} \frac{|h_{ij}|^2 E_s}{2N_0}, \quad (17)$$

where M_R is the number of receive antennas. Such additive property of SNRs suggests the use of the *moment generating function* (MGF) method for computation of the symbol error probability of different modulation schemes [20]. The MGF for a nonnegative random variable γ with pdf $p_\gamma(\gamma), \gamma \geq 0$, is defined as

$$\mathcal{M}(s) = \int_0^\infty p_\gamma(\gamma) e^{s\gamma} d\gamma. \quad (18)$$

The idea behind the MGF approach is to express the probability of error in AWGN for the modulation of interest as an exponential function of γ. For instance, let us suppose that the probability of symbol error P_s in AWGN for the modulation of interest is expressed in the form

$$P_s(\gamma) = c_1 e^{-c_2 \gamma}, \quad (19)$$

where c_1 and c_2 are constants. Hence, because the average probability of symbol error is computed by integrating the error probability in AWGN over the fading distribution [20], we have

$$\overline{P}_s = \int_0^\infty P_s(\gamma) p_\gamma(\gamma) d\gamma = \int_0^\infty c_1 e^{-c_2\gamma} p_\gamma(\gamma) d\gamma$$
$$= c_1 \mathcal{M}(-c_2), \quad (20)$$

where $\mathcal{M}(-c_2)$ is the MGF of γ evaluated at $-c_2$.

Given that, the symbol error probability of the Alamouti scheme becomes particularly simple if it is assumed that the fading paths are independent but not necessarily identically distributed. In this case, the branch SNRs are independent and the joint pdf of γ becomes a product of the individual pdfs, i.e., $p_{\gamma_1,\ldots,\gamma_M}(\gamma_1, \ldots, \gamma_{2M}) = p_{\gamma_1}(\gamma_1) \cdots p_{\gamma_{2M}}(\gamma_{2M})$. Using this factorization and substituting $\gamma = \gamma_1 + \ldots + \gamma_{2M}$ in Eq. (20) yields

$$\overline{P}_s = c_1 \int_0^\infty \cdots \int_0^\infty \exp\left[-c_2 \left(\sum_{i=1}^{2M} \gamma_i \right) \right] \prod_{i=1}^{2M} p_{\gamma_i}(\gamma_i) d\gamma_i$$
$$= c_1 \prod_{i=1}^{2M} \int_0^\infty e^{-c_2 \gamma_i} p_{\gamma_i}(\gamma_i) d\gamma_i$$
$$= c_1 \prod_{i=1}^{2M} \mathcal{M}_{\gamma_i}(-c_2) \quad (21)$$

[2]The same additive property of SNRs is observed in receiver diversity with maximal ratio combining (MRC) [20].

For instance, the symbol error probability for DBPSK under AWGN is $P_s = P_b(\gamma_b) = \exp(-\gamma_b)/2$, i.e., $c_1 = 0.5$ and $c_2 = 1$. Hence, the average probability of bit error under DBPSK is given by

$$\overline{P}_b = \frac{1}{2}\prod_{i=1}^{2M}\mathcal{M}_{\gamma_i}(-1). \tag{22}$$

For Rician fading, the moment generating function is given by [20]

$$\mathcal{M}_\gamma(s) = \frac{1+K}{1+K-s\overline{\gamma}}\exp\left[\frac{Ks\overline{\gamma}}{1+K-s\overline{\gamma}}\right]. \tag{23}$$

Substituting Eq. (23) into Eq. (22) we obtain the average probability of bit error for the Alamouti scheme with two transmit antennas and M receive antennas in the case of DBPSK modulation under Rician fading, which is given by

$$\overline{P}_b = \frac{1}{2}\left[\frac{1+K}{1+K+\overline{\gamma}}\right]^{2M}\exp\left[\frac{-2MK\overline{\gamma}}{1+K+\overline{\gamma}}\right]. \tag{24}$$

Following the same approach, one can obtain average error probabilities for many other modulations schemes under multipath fading [20].

As a final note, the same development can be used when considering the SINR of Eq. (16). In this case, as usual, the aggregate MAI is assumed to be Gaussian-distributed, with the mean and covariance matrix as computed before, and assuming that the channel gains in the denominator of Eq. (16) correspond to *average channel gains*, which are nothing but, the channel gains due to path-loss propagation effects.

IV. Modeling Ad Hoc Networks

Given analytical models for the PHY and MAC layers, we want to express network performance as a result of the individual PHY/MAC-layer dynamics at each node in the network, which, fundamentally, depends on how the nodes interact and interfere with each other's dynamics. For this purpose, we make use of the general modeling framework for multihop ad hoc networks we originally introduced in [12] and [13], with the new features summarized in Section I. In the following, we give a brief overview of the main characteristics of our modeling approach, referring the reader to [13] for more details.

Our modeling approach focuses on the essential functionalities provided by the PHY and MAC layers, as well as their interaction. On the one hand, the MAC layer provides a scheduling discipline for nodes to access the shared channel(s), and this discipline renders probabilities with which nodes will attempt to transmit. On the other hand, the PHY layer encodes information attempting to ensure that the transmitted frames are received correctly; the likelihood with which a transmission attempt initiated by the MAC is successful depends on how well the signaling used defends against channel impairments (establishing thus, the interdependency between both layers).

In the specific case where a reliable delivery service is required at the MAC layer, a node retransmits a frame according to some specific rule until the frame is successfully transmitted or discarded after a certain number of failed attempts. In this process, the MAC protocol adjusts its behavior dynamically, according to some type of feedback information that it acquires during the attempts to transmit a particular frame. Ideally, the MAC protocol uses this feedback information to schedule retransmissions in a way that the number of unsuccessful transmissions is minimized.

Let $\boldsymbol{v}_i(t)$ denote a *vector of feedback variables* used by a particular MAC protocol at each node $i \in V$ at time t (where V represents the set of nodes in the network). Because we are proposing a probabilistic model, we assume that $\boldsymbol{v}_i(t)$ contains *feedback probabilities*, i.e., probabilities of events whose outcomes are important feedback information to the MAC protocol in place. In this sense, a MAC protocol can be seen as a *stochastic dynamic system* whose feedback information is the vector of feedback probabilities $\boldsymbol{v}_i(t)$, and the corresponding output is the *scheduling rate* $\tau_i(t),\ i \in V$. Therefore, the MAC operation can be represented by some function that maps the feedback input $\boldsymbol{v}_i(t)$ into the desired outputs $\tau_i(t),\ i \in V$. Assuming a steady-state operation [12], the MAC functionality can be represented by some time-invariant (linear or non-linear) function $h_i(\cdot)$ as follows

$$\tau_i = h_i(\boldsymbol{v}_i),\ i \in V, \tag{25}$$

where the subscript i in $h_i(\cdot)$ denotes the node-specific instantiation of the MAC protocol in use. Let $\boldsymbol{v}_i = [v_{i1}\ v_{i2}\ \ldots\ v_{il}]^T$ be a vector of l feedback variables (the symbol T indicates the transpose operation). If the first n derivatives of $h_i(\boldsymbol{v}_i)$ at a point $\boldsymbol{v}_i^o = [v_{i1}^o\ v_{i2}^o\ \ldots\ v_{il}^o]^T$ are continuous, then $h_i(\boldsymbol{v}_i)$ has a Taylor series at the point $\boldsymbol{v}_i^o = [v_{i1}^o\ v_{i2}^o\ \ldots\ v_{il}^o]^T$ given by

$$h_i(\boldsymbol{v}_i) = h_i(\boldsymbol{v}_i^o) + \sum_{k=1}^{l}\left.\frac{\partial h_i}{\partial v_{ik}}\right|_{\boldsymbol{v}_i=\boldsymbol{v}_i^o}(v_{ik}-v_{ik}^o) + \cdots \tag{26}$$

Hence, a first-order approximation of $h_i(\boldsymbol{v}_i)$ at point $\boldsymbol{v}_i^o = [v_{i1}^o\ v_{i2}^o\ \ldots\ v_{il}^o]^T$ is simply

$$\tau_i = h_i(\boldsymbol{v}_i) \approx a_{i0} + a_{i1}v_{i1} + a_{i2}v_{i2} + \ldots + a_{il}v_{il}, \tag{27}$$

where

$$a_{ik} = \left.\frac{\partial h_i}{\partial v_{ik}}\right|_{\boldsymbol{v}_i=\boldsymbol{v}_i^o} \quad \text{for} \quad k = 1, 2, \ldots, l, \tag{28}$$

and

$$a_{i0} = h_i(\boldsymbol{v}_i^o) - \sum_{k=1}^{l} v_{ik}^o \left.\frac{\partial h_i}{\partial v_{ik}}\right|_{\boldsymbol{v}_i=\boldsymbol{v}_i^o}. \tag{29}$$

Equations (27), (28), and (29) give us the transmission probability τ_i of every node $i \in V$ as a linear combination of each node's own feedback probabilities $v_{ik}, k = 1, 2, \ldots, l$. The number and nature of the feedback probabilities depend on the chosen MAC protocol and the scenarios investigated. For instance, one should expect τ_i to be a function of the steady-state probability that a packet is available at a node's input queue, i.e., that the queue is not empty. Consequently, τ_i should also be a function of the input data traffic distribution

at node $i \in V$. In the literature, however, the throughput of a packet-radio network is generally studied by assuming saturation at all nodes, i.e., all buffers are full [21]. In this case, one is normally concerned with the maximum throughput attainable by the network when all nodes are actively seeking access to the channel. Another example of feedback information that can be particularly important to carrier-sense based MAC protocols is the probability that the channel is idle. In such protocols, the node only attempts to transmit a frame if the channel is sensed idle. Otherwise, it refrains from transmit the frame.

As far as a reliable delivery service at a given MAC protocol is concerned (contention- or schedule-based MAC), the single most important feedback information is the *probability that a frame transmission is successful*. This is, in fact, the main information that the MAC protocol uses to schedule retransmissions and transmissions of new frames. This information is the key link between the PHY and MAC layers. How well the signaling used defends against channel impairments determines the evolution of the MAC protocol itself. Moreover, due to the inherent broadcast nature of wireless networks, this feedback probability depends on the activity of *every other node in the network*, which in turn depends on how well the PHY layer guarantees the minimum interference among simultaneous transmissions and how well the MAC protocol avoids the concurrent scheduling of potential interfering transmissions over the channel.

At the PHY layer, the successful reception of every bit of information transmitted by a node i to a node r is related to the *signal-to-interference-plus-noise density ratio* SINR_i^r at node r (assuming a spread-spectrum system), which is given by (using a conventional matched filter receiver):

$$\mathrm{SINR}_i^r = \frac{P_i^r L_i}{\sum_{\substack{j \in V \\ j \neq i}} \chi_j P_j^r + \sigma_r^2}, \tag{30}$$

where P_k^r denotes the received signal power at node r for a signal transmitted by node $k \in V$, L_i is the spreading gain (or bandwidth expansion factor) of the spread-spectrum system, σ_r^2 is the background or thermal noise power at the front end of the receiver r, and χ_j is an on/off indicator, i.e.,

$$\chi_j = \begin{cases} 1, & \text{if } j \text{ transmits at the same time,} \\ 0, & \text{otherwise.} \end{cases} \tag{31}$$

Each time node i transmits a frame to node r, the (instantaneous) multiple access interference (MAI) level at node r depends on which nodes in V are transmitting concurrently with node i, as indicated by the variable χ_j, a Bernoulli-distributed random variable with probability τ_j, the probability that node j transmits a frame at any time, according to the MAC protocol in place. Because $|V| = n$, there are exactly 2^{n-2} combinations of potential active nodes (interferers) transmitting concurrently with i (excluding both transmitter i and receiver r). Let $\{c_{ik}^r\}_{k=1,\ldots,2^{n-2}}$ denote the set of such combinations, and $\mathcal{C}_i^r$ be a random variable that indicates the occurrence of a specific combination c_{ik}^r of interferers. For simplicity, we also assume that, when node i transmits a frame to node r, the set of interferers remains the same throughout the entire transmission of the frame. In reality, of course, some nodes may become active or inactive during the course of a frame transmission. However, this assumption is reasonable if frames are short and transmission rates are high. Consequently, during the reception of a frame—and for a fixed set of interferers—the bit-to-bit variations that may occur in SINR_i^r results from RF propagation effects only. Typically, the received signal powers P_i^r are subject to large-scale path loss, shadowing, and small-scaling multipath fading.

Therefore, depending on which nodes are active at the time node i transmits a frame to node r, there will be different values for the SINR and, consequently, different bit-error probabilities. Consequently, the frame error probabilities must be known for *every possible combination* $\{c_{ik}^r\}_{k=1,\ldots,2^{n-2}}$, which depends on the *joint probabilities* of occurrence of all the combinations $\{c_{ik}^r\}_{k=1,\ldots,2^{n-2}}$. The exact functional form of the joint probabilities depends on the specific MAC protocol in use. However, finding exact functional forms is inherently a difficult task, given the complexity of the interactions among the nodes, specially under multihop scenarios. Moreover, because the number of possible combinations of active interferers increases exponentially with the number of nodes, computing the probabilities of all the joint events becomes prohibitive with just a few tens of nodes.

In [13] we succeed in obtaining a linear approximation to the computation of the successful frame transmission probabilities (and subsequent handshake probabilities) for *any* multihop ad hoc network by taking advantage of the *necessary* behavior of *any* MAC protocol. In the linear approximation, the successful frame/handshake probabilities are expressed as functions of *all* the other nodes' transmission probabilities. Along the same lines, other feedback variables (e.g., the probability that the channel is "idle") are also expressed as functions of other nodes' transmission probabilities. Once all the feedback probabilities are expressed as functions of other nodes' transmission probabilities, a linear system of equations can be constructed from Eq. (27) to solve each node's transmission probability. From that, one can obtain many performance metrics (per node) such as the service time and throughput.

V. Modeling the IEEE 802.11 DCF MAC

In the recent past, there have been several attempts to model the IEEE 802.11 DCF MAC [9]. One of the most prominent works is the one by Bianchi [19], who presented a way to evaluate the saturation throughput of fully-connected networks based on the modeling of the binary exponential backoff algorithm used in the IEEE 802.11 DCF MAC. Bianchi modeled the backoff time counter operation as a bi-dimensional discrete-time Markov chain, assuming that each frame "collides" with a constant and independent probability p at each transmission attempt, regardless of the number of retransmissions already undertaken. This probability was named the *conditional collision probability*, meaning the probability of a collision experienced by a frame being transmitted on the

channel. From the Markov chain, one can obtain the steady-state probability τ that a node transmits a frame at any time as a function of the conditional collision probability p and some parameters of the IEEE 802.11 DCF backoff algorithm.

Building upon Bianchi's model, some works have tried to deal with other aspects of the IEEE 802.11 DCF not previously considered. Ziouva and Antonakopoulos [22] provided a general model for CSMA/CA protocols based on Bianchi's model. They assumed a backoff algorithm close to the one in the 802.11, and included the "freezing" activity of the 802.11 backoff algorithm, defining the probability of *detecting the channel busy*. Because their model targeted general CSMA/CA protocols, their Markov chain does not accurately reflects the IEEE 802.11 DCF operation. Ergen and Varaiya [23] followed Ziouva's approach with respect to the impact of the carrier sensing mechanism, and focused on the IEEE 802.11 itself. In their model, however, they make the very simplifying assumption that the conditional collision probability is *equal* to the probability of detecting the channel busy. The model by Ziouva and Antonakopoulos [22] makes this same simplifying assumption, particularly when the number of nodes in the network is large.

One drawback of these models (including Bianchi's) is the fact that they do not consider the finite retry limits of the IEEE 802.11 DCF, which proposes that DATA and RTS frames must be retransmitted a finite number of times. Instead, they all assume that frames are retransmitted *infinitely* in time, until they are successfully transmitted. Wu et. al. [24] incorporated the finite retry limit into Bianchi's model. On the other hand, Wu's model did not attempt to model the impact of the carrier sense mechanism.

A major limitation of all the aforementioned models is the fact that they implicitly assume a fully-connected segment of network under perfect channel conditions (i.e., no hidden terminal problems, no PHY-layer aspects, etc.). Consequently, by defining a "collision probability," they assume that all frames received at the same time "collide" and, therefore, they are all lost. By doing so, they assume that all "collisions" are restricted to RTS frames only, and therefore disregard the possibility of errors in the CTS, DATA or ACK frames. In fact, by its very definition, all the previous models mistakenly define p, which should actually be referred as the *probability of a failed handshake*, since a sender's frame could still be correctly received at the receiver's side, but not its acknowledgment. In addition, it is not true, for instance, that the probability of a failed handshake is the same (or similar) to the probability of detecting the channel busy. Each of these probabilities reflect totally different phenomena at the PHY layer. Detecting that a channel is busy only requires that some energy level be perceived at a node (as a result of some transmission(s)). On the other hand, transmission errors are related to a more complex process, and deals with the ability of the nodes to correctly receive a frame, which depends on many PHY-layer parameters such as the modulation/demodulation scheme, receiver design, and the like.

If errors in both control and data frames are to be considered, then the modeling of the IEEE 802.11 backoff operation needs to be modified. This is because all previous work has disregarded the *two retry counters* defined by the standard [9]: the STA long retry counter (SLRC) and the STA short retry counter (SSRC). The SSRC is associated with the RTS frame, and the SLRC is associated with the DATA frame[3]. The SSRC (SLRC) is incremented whenever an RTS (DATA) frame is unsuccessfully transmitted. The SSRC (SLRC) is reset to 0 whenever a CTS (ACK) frame is received in response to an RTS (DATA) frame. Therefore, even though the SRRC may be reset after a successful RTS transmission, the subsequent DATA frame transmission may be unsuccessful, leading, instead, to an *increment* of the SLRC.

According to the standard [9], the contention window size is reset to its minimum value only after a successful DATA frame transmission occur or when the SLRC or SSRC reach their maximum values—*but never after a successful RTS transmission*. In previous models, the CTS, DATA, and ACK frames were all assumed to be error-free after a successful RTS transmission, implying that a reset of SRRC would necessarily lead to a reset of the contention window size (since the SLRC would never be incremented). Therefore, in previous works, the contention window size was solely controlled by the number of unsuccessful RTS transmissions.

For a faithful modeling of the IEEE 802.11 DCF MAC, one needs to consider both SSRC and SLRC retry counters. Unfortunately, following the modeling approach used by Bianchi renders a four-dimensional Markov chain to cover all possible states of the binary exponential backoff algorithm. To make things simpler—while still considering the impact of errors in both control and data frames—we consider a small simplification of the original IEEE 802.11 DCF MAC by defining a *single* retry counter RC. The RC will be incremented every time an RTS or DATA frame is unsuccessfully transmitted, i.e., when the CTS/ACK are not received within a timeout or when they are received with errors. Likewise, the RC and the contention window size will be reset only when either a DATA frame is successfully transmitted or when RC reaches its maximum value. As in the standard, we allow the contention window to increment up to a maximum value, after which it remains at this value until it is reset. With this small simplification, we are able to model the IEEE 802.11 DCF MAC using only a two-dimensional Markov chain, as described next.

Let $b_j(t)$ be the stochastic process representing the backoff time counter for a node $j \in V$ at a time t, and $s_j(t)$ be the stochastic process representing j's backoff stage at time t, where $s_j(t) \in [0, M]$, and M is the maximum backoff stage (i.e., the maximum value the retry counter RC can assume). Hence, $b_j(t) \in [0, W_{s_j(t)} - 1]$, where

$$W_{s_j(t)} = \begin{cases} 2^{s_j(t)} W_{\min} & \text{if} \quad 0 \leq s_j(t) < m \\ 2^m W_{\min} & \text{if} \quad m \leq s_j(t) \leq M. \end{cases} \tag{32}$$

Let us assume that the RTS/CTS handshake fails with a con-

[3]If this frame is bigger than a certain user-defined threshold.

stant and independent probability p_j, and that the DATA/ACK handshake fails with a constant and independent probability d_j, both regardless of the number of retransmissions experienced. Also, let us assume that a node detects that the channel is busy with a constant and independent probability g_j. Note that these independence assumptions are with respect to the *number of retransmissions*, but p_j, d_j, and g_j are *dependent on PHY-layer aspects*, and are computed according to the developments in Section IV. Under these conditions, the process $\{s_j(t), b_j(t)\}$ can be modeled with the discrete-time Markov chain depicted in Fig. 1.

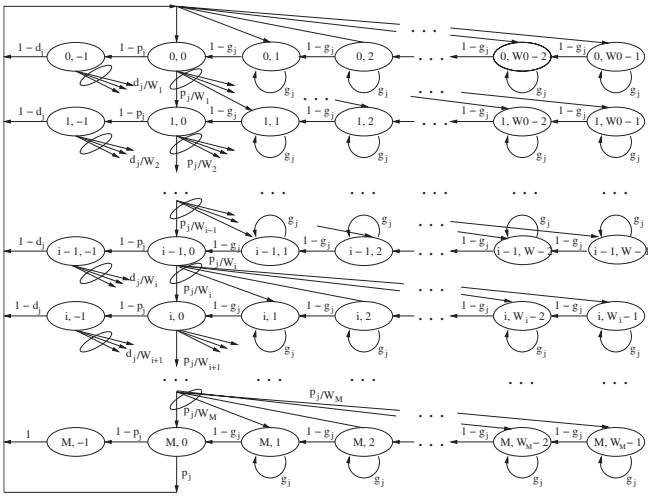

Fig. 1. Markov model for the *modified* binary exponential backoff algorithm based on the IEEE 802.11 DCF MAC. Losses in both control and data frames taken into account.

Following Bianchi's work [19], we adopt the notation $P\{i_1, k_1|i_0, k_0\} = P\{s(t+1) = i_1, b(t+1) = k_1|s(t) = i_0, b(t) = k_0\}$. From the above Markov chain, the only non-null one-step transition probabilities are

$$
\begin{array}{lll}
P\{i,k|i,k+1\} = 1-g_j, & k \in [0, W_i - 2], & i \in [0, M] \\
P\{i,k|i,k\} = g_j, & k \in [1, W_i - 1], & i \in [0, M] \\
P\{i,-1|i,0\} = 1-p_j, & & i \in [0, M] \\
P\{i,k|i-1,0\} = \frac{p_j}{W_i}, & k \in [0, W_i - 1], & i \in [1, M] \\
P\{i,k|i-1,-1\} = \frac{d_j}{W_i}, & k \in [0, W_i - 1], & i \in [1, M] \\
P\{0,k|i,-1\} = \frac{(1-d_j)}{W_0}, & k \in [0, W_0 - 1], & i \in [0, M-1] \\
P\{0,k|M,0\} = \frac{p_j}{W_0}, & k \in [0, W_0 - 1] & \\
P\{0,k|M,-1\} = \frac{1}{W_0}, & k \in [0, W_0 - 1]. &
\end{array}
$$

The first and second equations indicate that the backoff counter is decremented if the channel is sensed idle (with probability $1-g_j$), and frozen if the channel is sensed busy (with probability g_j). The third equation indicates that a successful handshake of control frames took place and the node is ready to send its DATA frame. The next equation indicates that, after an unsuccessful handshake of control frames (RTS/CTS) at stage $i-1$, a backoff interval is uniformly chosen within the interval $[0, W_i - 1]$ for the next stage i. The fourth equation indicates that the transmission of DATA frame failed at stage $i-1$, and a backoff interval is uniformly chosen within the interval $[0, W_i - 1]$. The fifth equation indicates that a DATA frame was transmitted successfully and a new frame transmission starts at backoff stage 0 with a backoff window uniformly chosen within the interval $[0, W_0 - 1]$. The next equation indicates that a handshake of control packets failed and the number of allowed retransmissions reached its maximum. Hence, the DATA frame is discarded and a new one is picked at the head of the node's queue. A new frame transmission starts at backoff stage zero with a backoff window uniformly chosen within the interval $[0, W_0 - 1]$. The last equation describes that either a DATA frame transmission was successful or it failed. In either case, a new frame starts at backoff stage 0 with a backoff window uniformly chosen within the interval $[0, W_0 - 1]$.

Let $b_{i,k} = \lim_{t\to\infty} P\{s(t) = i, b(t) = k\}, i \in [0, M], k \in [0, W_i - 1]$ be the stationary distribution of the Markov chain. First, we note that

$$b_{i,0} = p_j\, b_{i-1,0} + d_j\, b_{i-1,-1}, \quad 1 \le i \le M. \tag{33}$$

However, given that $b_{i-1,-1} = (1-p_j) b_{i-1,0}$, we have

$$b_{i,0} = [p_j + d_j(1-p_j)]\, b_{i-1,0}, \tag{34}$$

which leads to

$$b_{i,0} = [p_j + d_j(1-p_j)]^i\, b_{0,0}, \quad 0 \le i \le M. \tag{35}$$

For $i = 0$ and $k \in [1, W_0 - 1]$,

$$b_{0,k} = \frac{W_0 - k}{(1-g_j)W_0} \sum_{l=0}^{M-1} (1-p_j)(1-d_j) b_{l,0} + b_{M,0}, \tag{36}$$

whereas for $i \neq 0$ and $k \in [1, W_i - 1]$,

$$b_{i,k} = \frac{W_i - k}{(1-g_j)W_i} [p_j + d_j(1-p_j)]\; b_{i-1,0}, i \in [1, M]. \tag{37}$$

From Eq. (34), and by noting that $b_{0,0} = \sum_{l=0}^{M-1}(1-p_j)(1-d_j)b_{l,0} + b_{M,0}$, Eqs. (36) and (37) can be rewritten as

$$b_{i,k} = \frac{W_i - k}{(1-g_j)W_i} [p_j + d_j(1-p_j)]^i\; b_{0,0}, \tag{38}$$

for $i \in [0, M]$ and $k \in [1, W_i - 1]$. Therefore, all values of $b_{i,k}$ can be expressed as functions of $b_{0,0}$, whose value can be found from the normalization condition $\sum_{i=0}^{M} \sum_{k=0}^{W_i - 1} b_{i,k} = 1$, yielding

$$b_{0,0} = \frac{2(1-g_j)(1-a_j)(1-2a_j)}{(1-a_j^{M+1})(1-2a_j)(1-2g_j) + \kappa W}, \tag{39}$$

where $a_j = p_j + d_j(1-p_j)$, and $\kappa = (1-a_j)\left[1-(2a_j)^{M+1}\right]$ if $m = M$, and $\kappa = 1 - a_j\{1 + (2a_j)^m[1 + a_j^{M-m}(1-2a_j)]\}$ if $m < M$.

A node initiates a handshake when it attempts to send an RTS, i.e., when it reaches the states $b_{i,0},\ i \in [0, M]$. Therefore, the probability τ_j that node j attempts to initiate a handshake is obtained by taking $\tau_j = \sum_{i=0}^{M} b_{i,0}$, which is given by

$$\tau_j = \frac{2(1-g_j)(1-a_j^{M+1})(1-2a_j)}{(1-a_j^{M+1})(1-2a_j)(1-2g_j) + \kappa W}, \tag{40}$$

with κ assuming the same values as before depending on whether $m \leq M$. It is interesting to note that, if $M \to \infty$, then $g_j = 0$, $d_j = 0$, and the Markov chain in Fig. (1) reduces to the one used by Bianchi [19] for the case when $m < M$. Accordingly, by making $M \to \infty$, we have $g_j = 0$, and $d_j = 0$ in Eq. (40), and we obtain the same expression derived by Bianchi [19].

Given the expression for the transmission probability τ_j, we can obtain its linear approximation by following the steps in Section IV. By defining $q_j^{rts} = 1 - p_j$ and $q_j^{dat} = 1 - d_j$, the vector $\boldsymbol{v}_j$ of feedback probabilities is $\boldsymbol{v}_j = [q_j^{rts}\, q_j^{dat}\, g_j]^T$, and the linear approximation of τ_j is given by

$$\tau_j = \frac{2(1-W)}{(W+1)^2} + \frac{2Wq_j^{rts}}{(W+1)^2} + \frac{2Wq_j^{dat}}{(W+1)^2} - \frac{2(W-1)g_j}{(W+1)^2}, \tag{41}$$

which is in the linear form of Eq. (27) with $a_{j0} = 2(1 - W)/(W+1)^2, a_{j1} = a_{j2} = 2W/(W+1)^2$, and $a_{j3} = 2(W - 1)/(W+1)^2$. The computation of $\boldsymbol{v}_j = [q_j^{rts}\, q_j^{dat}\, g_j]^T$ follows the developments introduced in Section IV and in [13].

VI. Model Validation

We implemented the analytical model in Matlab™ 7.0 [25], and conducted discrete-event simulations in Qualnet™ v3.5 [26]. The selected path loss propagation model is the two-ray ground reflection model. No multipath fading and shadowing is considered in this validation. Bit errors are treated independently, as it is done in Qualnet™. Nodes are randomly placed in an area of 1000×1000 m. For the physical layer, we use the direct sequence spread spectrum (DSSS) IEEE 802.11 PHY, with a raw bit rate of 1 Mbps under DBPSK modulation. Table I summarizes the rest of the parameters used for the PHY and MAC layers.

TABLE I
MAC- and PHY-Layer Parameters

MAC		PHY	
$W_{\min}$	32	Temperature (Kelvin)	290
$W_{\max}$	1024	Noise factor	10
MAC Header (bytes)	34	Transmission power (dBm)	10
ACK (bytes)	38	Receive Sensitivity (dBm)	-87.039
CTS (bytes)	38	Receive Threshold (dBm)	-76.067
RTS (bytes)	44	Packet reception model	BER
Slot Time (μsec)	20	No Fading	
SIFS (μsec)	10		
DIFS (μsec)	50		

Each node has a single, one-hop receiver for its packets throughout the simulation time, to which it will send fixed-size packets of 1500 bytes (IP packet) generated from a CBR source. The source rate is high enough to saturate all nodes. Each simulation run corresponds to 5 minutes of data traffic, and the experiment is repeated for 20 seeds, with each trial corresponding to a different initial transmission time for each node. Initial transmission times are randomly chosen within the interval $[0,\, 0.01]$ s. This is done to allow the IEEE 802.11 exponential backoff algorithm to be triggered at different time instants at each node, so that different state evolutions occur within the same topology. Figure 2 shows the average throughput results computed for 10 random topologies with 100 nodes each. As we can see, the model is able to predict the average throughput very accurately, indicating that, even though we have assumed a simplification of the IEEE 802.11 in order to model it, the results indicate that the difference is not significant and, as a result, we can use this model for purposes of performance evaluation of the IEEE 802.11 DCF MAC.

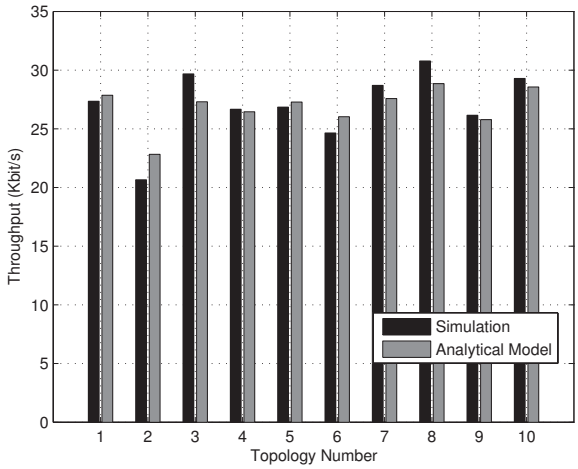

Fig. 2. Average network throughput for 10 random topologies with 100 nodes each.

VII. Performance of MIMO Ad Hoc Networks

In this Section, we evaluate the performance of ad hoc networks that employ the Alamouti scheme at the physical layer and operate with the modified IEEE 802.11 DCF MAC described before. We investigate both MISO and MIMO ad hoc networks by taking advantage of the flexibility of the Alamouti scheme (it works with any number M of receive antennas, as explained in Section III). Table II contains the configurations of the antenna systems we study. For the MISO case, we assume that all nodes are equipped with two antennas. In this case, both antennas are used during transmission (necessary for the Alamouti scheme) and, during reception, only the signals arriving at one of the antennas are conveyed to the appropriate decoding/demodulation stages. For the MIMO cases, the opposite applies, i.e., all nodes are equipped with $M \geq 2$ antennas, but only two of them are used during transmission, whereas all antennas are used during reception. The performance of both MISO and MIMO networks are compared with the basic SISO network (nodes equipped with a single antenna). In the following, we will refer to a network with N transmit antennas and M receive antennas as an $N \times M$ MISO/MIMO network (depending on the values of N and M).

One of the advantages of MIMO systems is to combat time-varying multipath fading. For our study, we assume a multipath fading following a Rician model [20]. We choose the Rician model because it is appropriate for scenarios where there

TABLE II

ANTENNA CONFIGURATIONS USED FOR PERFORMANCE EVALUATION

System	N. of Transmit Antennas	N. of Receive Antennas
MISO	2	1
MIMO	2	2
MIMO	2	4
MIMO	2	6

exists both line-of-sight (LOS) and non-line-of-sight (NLOS) signals. The key parameter of the Rician distribution is the K parameter, which expresses the ratio of the power of the LOS signal to the power of the NLOS signals. A small value of K indicates a rich scattering environment with a weak LOS signal (strong fading). A large value of K indicates a decrease in multipath propagation and, therefore, weak fading. We assume that fading is frequency flat and independent at each path. Thus, we can use the bit-error computation procedures presented in Section III-C.

For the numerical results, we use the same setup and PHY/MAC parameters as described in Section VI, with the exception of the inclusion of multipath fading. We compute the average network throughput over 10 random topologies with 100 nodes each, for different values of the Rician parameter K and for the antenna systems indicated in Table II. Figure 3 shows the numerical results. The bars in the graph indicate the standard deviation of the computed averages. As we can see, the use of the Alamouti scheme does improve performance significantly, especially when fading is strong (small values of K). For instance, the gains in average throughput of the 2×6 MIMO over the simplest SISO network are almost 400% when $K = 5$. Improvements in throughput are perceived even for the basic MISO configuration, which improves throughput over SISO in more than 200% under strong fading, and about 125% without much fading (large K).

Another important aspect to observe it that, as the number of receive antennas increases ($M > 2$), the relative gains in average throughput diminishes with respect to the previous configuration. Therefore, we observe that adding more antennas at each node does not give a linear increase in performance. As the number of antennas increases, the errors in the channel are better combated, and throughput becomes basically bounded by the degree of contention in the network. In other words, it is the MAC layer that limits the achievable throughput once the PHY layer attains its best performance. Such results are expected, because the Alamouti scheme is a *transmitter diversity* scheme. In other words, it was not designed to provide data rate increases (*capacity gains*) through spatial multiplexing. Instead, it provides a more robust channel through *diversity* and *array* gains, as explained in Section III-A.

The above results suggest that the use (or not) of more antennas depends on the amount of contention in place, which, in turn, depends on the total number of nodes, their distribution in the terrain, and the efficiency of the underlying MAC protocol in scheduling each node's transmissions. For the scenarios we studied, it seems that the best trade off that

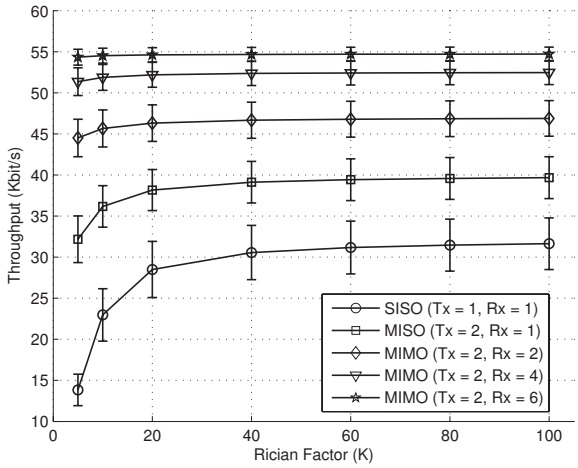

Fig. 3. Average network throughput versus the value of the Rician parameter K for different antenna systems. The results compare MISO and MIMO Alamouti-enabled 802.11 ad hoc networks with SISO 802.11 ad hoc networks.

can achieved between the number of antennas and the system complexity is the 2×2 MIMO configuration. Using four or six antennas does increase throughput, but the relative gains are not significant enough to justify the added system complexity. At the same time, the MISO network already has 2 antennas at each node, and the cost to implement a 2×2 MIMO network is just the extra internal processing of the signals captured by the second antenna already in place.

VIII. CONCLUSIONS

This paper presented the first analytical model for wireless ad hoc networks equipped with multiple-input multiple-output (MIMO) radios using space-time coding (STC) that considered the impact of the underlying radio-based topology on network performance. In particular, we considered the application of space-time block coding (STBC) in the form of a transmitter diversity technique known as the "Alamouti scheme." We derived the effective signal-to-interference-plus-noise density ratio (SINR) of the Alamouti scheme under multiple access interference (MAI), and we proposed the moment generating function (MGF) method to derive closed-form expressions for its symbol error probability under different modulation schemes when fading paths are independent but not necessarily identically distributed.

The impact of the Alamouti scheme on IEEE 802.11 ad hoc networks was studied by introducing a new analytical model for the IEEE 802.11 DCF MAC. The model we introduced takes into account the impact of errors in both control and data frames, the carrier-sensing activity, and the finite-retry limit of frame retransmissions. The PHY- and MAC-layer models that we developed were incorporated into our previously-designed analytical model for wireless ad hoc networks that is able to capture the interactions between both layers and to take into account the radio connectivity among the nodes—all conveniently conveyed through the use of *interference matrices*.

We studied the performance of the Alamouti scheme in IEEE 802.11 ad hoc networks by comparing the relative gains in performance between SISO, MISO, and MIMO systems. From our results, we found that the Alamouti scheme does improve performance of IEEE 802.11 ad hoc networks, especially in environments where multipath fading effects are severe. In addition, we found that as the number of receive antennas increase, the relative gains in performance decrease, being limited by the degree of contention in the network. For this reason, there is an inherent trade-off between performance and system complexity when choosing the appropriate number of receive antennas.

IX. Acknowledgments

This work was supported in part by the Baskin Chair of Computer Engineering at UCSC, the UCOP CLC under Grant SC-05-33, the U.S. Army Research Office under grants No. W911NF-04-1-0224 and W911NF-05-1-0246, and CAPES/Brazil. Any opinions, findings, and conclusions are those of the authors and do not necessarily reflect the views of the funding agencies.

References

[1] J. Winters, "On the capacity of radio communication systems with diversity in a rayleigh fading environment," *IEEE Journal on Selected Areas in Communications*, vol. SAC-5, pp. 871–878, June 1987.

[2] G. Foschini, "Layered space-time architecture for wireless communication in fading environments when using multi-element antennas," *Bell Labs Technical Journal*, pp. 41–59, 1996.

[3] G. Foschini and M. Gans, "On limits of wireless communications in a fading environment when using multiple antennas," *Wireless Personal Communications*, vol. 6, pp. 311–355, 1998.

[4] E. Telatar, "Capacity of multi-antenna gaussian channels," *European Trans. on Telecomm.*, vol. 10, pp. 585–596, 1999.

[5] D. Gesbert, M. Shafi, D. Shiu, P. Smith, and A. Naguib, "From theory to practice: An overview of MIMO space-time coded wireless systems," *IEEE Journal on Selected Areas in Communications*, vol. 21, no. 3, pp. 281–302, April 2003.

[6] A. Naguib, N. Seshadri, and A. Calderbank, "Increasing data rate over wireless channels," *IEEE Signal Processing Magazine*, pp. 76–92, May 2000.

[7] V. Tarokh, N. Seshadri, and A. Calderbank, "Space-time codes for high data rate wireless communications: Performance criterion and code construction," *IEEE Trans. Information Theory*, vol. 44, no. 2, pp. 744–765, March 1998.

[8] B. Vucetic and J. Yuan, *Space-Time Coding*, John Wiley & Sons Ltd., 2003.

[9] *IEEE Standard for Wireless LAN Medium Access Control (MAC) and Physical Layer (PHY) Specifications*, Nov 1997, P802.11.

[10] V. Tarokh, N. Seshadri, and A. Calderbank, "Space-time block codes from orthogonal designs," *IEEE Trans. Information Theory*, vol. 45, no. 5, pp. 1456–1467, July 1999.

[11] S. Alamouti, "A simple transmit diversity technique for wireless communications," *IEEE Journal on Selected Areas in Communications*, vol. 16, no. 8, pp. 1451–1458, October 1998.

[12] M. M. Carvalho and J. J. Garcia-Luna-Aceves, "A scalable model for channel access protocols in multihop ad hoc networks," in *Proc. MobiCom*, Philadelphia, USA, September 2004, pp. 330–344.

[13] M. M. Carvalho and J. J. Garcia-Luna-Aceves, "Modeling wireless ad hoc networks with directional antennas," in *Proc. IEEE INFOCOM*, Barcelona, Spain, April 2006.

[14] K. Sundaresan, R. Sivakumar, M. Ingram, and T. Chang, "A fair medium access control protocol for ad-hoc networks with MIMO links," in *Proc. of IEEE INFOCOM*, Hong Kong, March 2004.

[15] T. Tang, M. Park, R. Heath, and S. Nettles, "A joint MIMO-OFDM transceiver and MAC design for mobile ad hoc networking," in *Proc. Int. Workshop on Wireless Ad-Hoc Networks (IWWAN)*, Oulu, Finland, May 2004.

[16] J. Park, A. Nandan, M. Gerla, and H. Lee, "SPACE-MAC: Enabling spatial reuse using MIMO channel-aware MAC," in *Proc. IEEE Int. Conf. Communications (ICC)*, Seoul, Korea, May 2005.

[17] A. Stamoulis and N. Al-Dhahir, "Impact of space-time block codes on 802.11 network throughput," *IEEE Trans. on Wireless Communications*, vol. 2, no. 5, pp. 1029–1039, September 2003.

[18] M. Hu and J. Zhang, "MIMO ad hoc networks: Medium access control, satuation throughput, and optimal hop distance," *Journal of Communications and Networks*, pp. 317–330, December 2004.

[19] G. Bianchi, "Performance analysis of the IEEE 802.11 distributed coordination function," *IEEE Journal on Selected Areas in Communications*, vol. 18, no. 3, pp. 535–547, March 2000.

[20] A. Goldsmith, *Wireless Communications*, Cambridge University Press, 2005.

[21] F. A. Tobagi, "Modeling and performance analysis of multihop packet radio networks," *Proc. IEEE*, vol. 75, no. 1, pp. 135–155, Jan 1987.

[22] E. Ziouva and T. Antonakopoulos, "CSMA/CA performance under high traffic conditions: throughput and delay analysis," *Computer Communications*, vol. 25, no. 3, pp. 313–321, 2002.

[23] M. Ergen, B. Dunbar, and P. Varaiya, "Throughput analysis of an extended service set in 802.11," in *Proc. GLOBECOM*, Dallas, USA, November 2004.

[24] H. Wu, Y. Peng, K. Long, S. Cheng, and J. Ma, "Performance of reliable transport protocol over IEEE 802.11 wireless LAN: Analysis and enhancement," in *Proc. INFOCOM*, New York, USA, June 2002.

[25] The MathWorks, Inc, *Matlab v.7.0*.

[26] Scalable Network Technologies, Inc, *Qualnet User's Manual Simulator, version 3.5*.